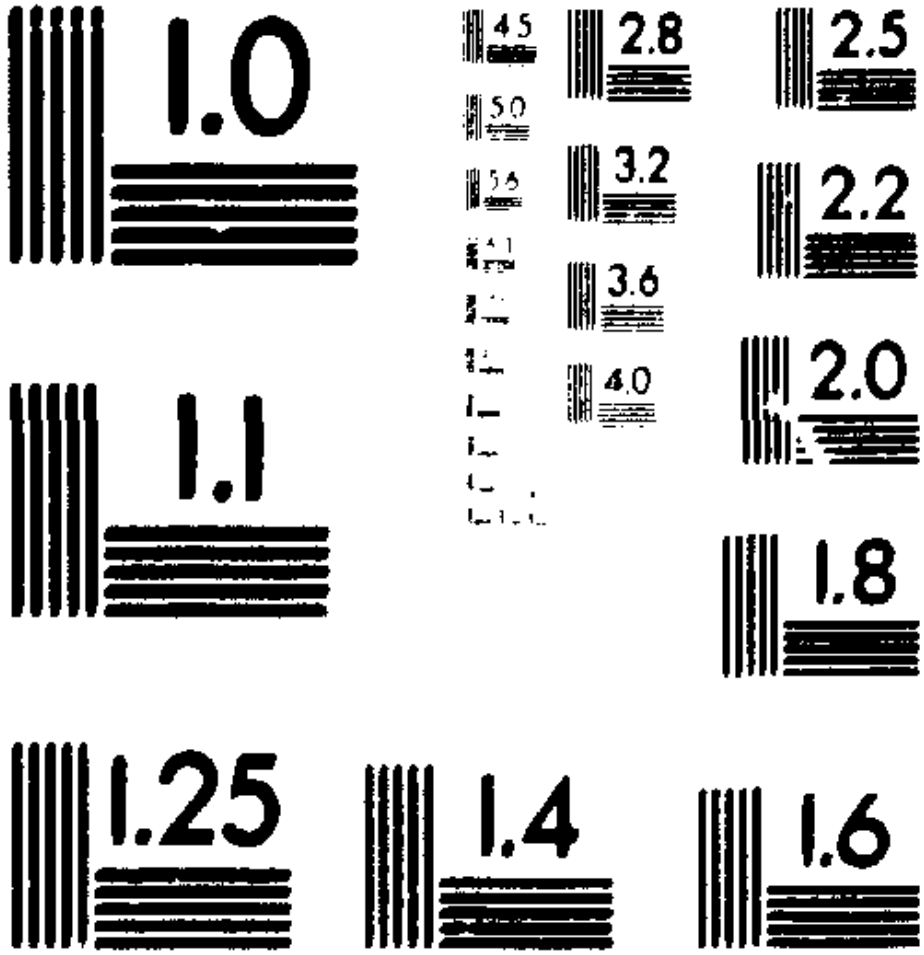

LNF-P-95-013.

LABORATORI NAZIONALI DI FRASCATI
SIS – Pubblicazioni

LNF-95/013 (P)
27 Marzo 1995

Influence of Interstitial Solutions (H,N) on the Cerium Electronic State in Ce–Fe Intermetallic Compounds: an X–ray Absorption Spectroscopy (XAS) Study

Jesús Chaboy
Instituto de Ciencia de Materiales de Aragón, CSIC–Universidad de Zaragoza,
50009 Zaragoza, Spain

Augusto Marcelli
NFN – Laboratori Nazionali di Frascati, P.O. Box 13, I-00044 Frascati, Italy

Latchezar Bozukov
Department Solid State Physics, Faculty of Physics, Sofia University, 1126 Sofia, Bulgary

Abstract

We present an x–ray absorption spectroscopy (XAS) investigation performed at the L–edges of the rare–earth and at the K–edge of iron in the R–Fe intermetallic compounds $(La,Ce)_2Fe_{14}BH_x$ and $Ce_2Fe_{17}(H,N)_x$, to elucidate the role of the interstitial doping into the electronic and magnetic properties of these systems. Comparison with x–ray circular magnetic dichroism (XCMD) experiments has been carried out to clarify the localization of 4f magnetic moment at the Ce sites upon hydriding. Both XAS and XCMD results evidence the interplay between the structural and magnetic changes, that are associated to the modification of the hybridization between the Fe(3d) and Ce(5d) bands.

PACS.: 78.70Dm, 78.20Ls, 61.10Lx, 75.30Mb, 75.50.Bb

Submitted to
Journal of Physics: Condensed Matter

I. INTRODUCTION

Since 1969 when Zijlstra and Westendorp reported the first observations about the ability of $SmCo_5$ to absorb large quantities of H_2 in a reversible way [1], a large body of research has been devoted regarding hydrogen absorption by intermetallic materials. As well as in the pioneer studies hydrogen was introduced by inadvertence, posterior interest was centered by the technological application of these materials [2]. Actually, it has been found that most of the members of the large group of intermetallic compounds formed among rare-earths, R, and elements of the d-transition series, M, can form stable hydrides and, very often, hydrogen absorption leads to strong changes of the macroscopic structural and magnetic properties of these materials. [2–6] Therefore, nowadays these studies have turned to understand not only the mechanism responsible for hydrogen absorption by intermetallic compounds but also to ascertain its effect on their magnetic, structural and electronic properties.

The interest has been recently renewed since the discovery of the $R_2Fe_{14}B$ materials. [7,8] The ternary compound $Nd_2Fe_{14}B$ exhibits superior high-performance permanent-magnet properties and economic advantages over the earlier Sm-Co materials. However, the range of temperature in which these new alloys allow technological applicability is strongly limited because ordering temperatures, T_c, are sufficiently low to render them unsuitable for some applications. [9–11] This characteristic is shared by all the known R-Fe binary alloys compounds, whose Curie temperatures are rather low. [12–14] The origin of the peculiar behavior of T_c is a matter of controversy. Several effects have been addressed as the responsible for this anomalous behavior: the more localized character of Fe moments as compared to Co and Ni moments [12]; the peculiar sensitivity of the Fe-Fe exchange interactions to the Fe-Fe separation [15,16]; local environment effects determining the molecular field coefficient, n_{FF}, that describes the Fe-Fe exchange interactions [16,17]; and the role of spin-fluctuations on T_c in itinerant electrons systems [18].

Hydrogen absorption is one of the most notable mechanisms able to achieve higher magnetic ordering temperature in these systems. The interstitial solution of H atoms leads to

both an increase in the crystal-cell volume, without a change in the crystal structure, and a rise of T_c. In the $R_2Fe_{14}BH_x$ series the relative volume expansion, $\Delta V/V$, varies between 2% and 6% and the increase on T_c varies between 40 and 50K depending on the nature of the rare-earth. [19–23] This behavior was interpreted in terms of the modification of the shortest Fe-Fe distances that according to the Slater-Neel curve can give rise to antiferromagnetic exchange interactions. [24] These findings have stimulated attempts to improve the magnetic properties of other R-Fe alloys, as the R_2Fe_{17} intermetallics, by using hydrogen absorption, that raises T_c by around 200 K in this series. [25–28] More recently, these studies have been extended to other interstitial solutions as C and N atoms. It has been found that in the R_2Fe_{17} intermetallics, interstitial C raises the Curie temperature up to 200 K [29–31], while the effect of nitrogen is even greater, producing increases of about 400 K. [32–34]

One of the most fascinating results obtained by studying the interstitial doping in R-3d intermetallics, is associated to the possibility to induce a change of valency on Ce atoms. [35] Indeed, such a behaviour should open a new route to develope a net Ce $4f$ magnetic moment in these materials. However, how the electronic structure of Ce ions in $Ce_2Fe_{14}B$ and Ce_2Fe_{17} systems is modified upon hydrogen(nitrogen) absorption is nowadays a matter of controversy. Severals authors have claimed for the existence of a Ce^{4+} to Ce^{3+} transition, i.e., from non-magnetic to magnetic configurations, taking place upon interstitial doping. This assignement has been proposed on the basis of the anomalous relative volume increase for the cerium compounds, that is significantly larger than those observed for the rest of the series. [28,35–43] The relative volume increase upon hydrogen uptake, $\Delta V/V$, is found to be 5.5 % and 6.2 % for $Ce_2Fe_{14}B$ and $Pr_2Fe_{14}B$ compounds, respectively. [21]. A similar trend has been also observed in the case of the $R_2Fe_{17}H_x$ series, in which $\Delta V/V$ is 5.3 % and 4.4 % for Ce and Pr, respectively. [36] Moreover, in the case of nitrogen absorption, this effect is even greater being $\Delta V/V$= 8.8 % and between 5.8 and 7.4 % for Ce_2Fe_{17} and Pr_2Fe_{17} compounds respectively. [34,36–38] However, although an earlier neutron diffraction investigation performed on $Ce_2Fe_{14}B$ and its hydride derivatives reported the development of a 2.2 μ_B magnetic moment at the Ce-4g site for deuterated samples, [35] this assignment has

not been confirmed neither by x-ray photoelectron spectroscopy [39] nor by x-ray absorption spectroscopy [44,45]. However, qualitative support to the neutron diffraction results has been addressed from recent analyses of XAS data. [46] Moreover, while in the case of the $CeFe_2$ system is well established that Ce ions develop a magnetic moment of $4f$ origin upon hydrogen absorption [45,47,48], in the case of Ce_2Fe_{17}, $Ce_2Fe_{14}B$ and their hydrides, XAS experiments do not support the interpretation based on the interplay between cerium valence and hydrogen absorption. [44,45,49–51]

In this work, we report an extensive x-ray absorption spectroscopy (XAS) study performed at the rare earth L-edges and at the Fe K-edge in the case of $La_2Fe_{14}B$, $Ce_2Fe_{14}B$ and Ce_2Fe_{17} systems and their hydrides derivatives. The aim of this work is to establish the modification of the electronic structure of Ce upon hydrogen absorption. This investigation has been extended to the study of the Ce_2Fe_{17} system upon nitrogen uptake. The valency state of cerium has been investigated by x-ray absorption near edge structure (XANES) at the Ce L_3-edge. In addition, measurements of the cerium L_1-edge and Fe K-edge XANES spectra have been performed to determine the modification of the local and partial density of states around the Fermi energy induced by interstitial doping. Such combined analysis shows electronic localization phenomena that address the change in the magnetic properties of the systems upon hydriding to the modification of the 3d(Fe)-5d(R) hybridization. To discuss the dynamics of Ce electronic state upon hydrogen (nitrogen) absorption in these iron-rich intermetallics compounds, XAS results are compared to x-ray circular magnetic dichroism (XCMD) experiments recently published. [49,52]

II. EXPERIMENTAL SETUP

Samples were prepared by arc-melting the starting elements (purity 99.9%) under purified Ar atmosphere. Both phase and structural analysis were performed on a standard x-ray diffractometer. The hydrogen (nitrogen) absorption-desorption properties were established according to the standard methods. [20,28,32]

XAS experiments have been performed at the Fe K-edge and at the $L_{1,3}$-edges of La and Ce in the case of $(La,Ce)_2Fe_{14}BH_x$, and $Ce_2Fe_{17}(H,N)_x$ systems (x being the maximum gas content). Several samples were measured in different experimental runs at the PULS synchrotron radiation facility of the Laboratori Nazionali di Frascati. The ADONE storage ring was operated at 1.5 GeV during dedicated beam time with an averaged current of 40 mA.

For these experiments fine powders of the material were homogeneously spread on an adhesive tape. Thickness and homogeneity of the samples were optimized to obtain the best signal to noise ratio using two layers of powdered material giving a total absorption jump, $\Delta\mu x$, ranging between 0.4 and 0.8 as a function of the absorption edge selected. Measurements were carried out at room temperature in the transmission mode, being the x-ray radiation monochromatized using a Si(111) channel-cut crystal. Both incident x-rays and transmitted through the sample were monitored by using two independent ionization chambers with N_2-Ar flowing gas mixture optimized for each energy range.

The absorption spectra were analyzed according to standard procedures [53]. The background contribution from lower energy absorption edges, $\mu_B(E)$, was approximated according to the Victoreen rule and subtracted from the experimental spectrum, $\mu(E)$. Spectra were then normalized to the absorption coefficient at high energy to eliminate thickness dependence. The energy origin E_0, corresponding to the continuum threshold, was defined to be at the inflection point of the absorption edge.

III. RESULTS AND DISCUSSION

A. Fe K-edge XANES spectra

The x-ray absorption spectrum is usually divided in three regions as a function of the kinetic energy of the photoelectron: the first part of the spectrum extending over about 10 eV, called edge-region; the region of the multiple scattering in the continuum, XANES;

and the region of single-scattering at higher energies, EXAFS. In the XANES and EXAFS regions, the photoelectron is scattered in the real space by neighboring atoms so that direct structural information, i.e., coordination geometry and bond angles, can be extracted from the absorption spectra. [54] On the contrary, the near-edge region of the spectrum carries information about the electronic state of the absorbing atom. Indeed, in the case of metals, in the region up to about 10 eV above the threshold, E_0, (i.e., the photon energy of the core excitation to the Fermi level) the photoelectrons are elastically scattered by the valence electrons. Therefore, the final states of the photoelectron should be described as unoccupied states close to the Fermi level and, because in metals the core-hole in the final state potential is fully screened by the valence electrons close to the Fermi level, the edge spectrum probes the unoccupied ground-state local and partial density of states.

The normalized XANES spectra recorded at the Fe K-edge in the case of $La_2Fe_{14}B$ and its hydride derivative are compared in Fig. 1. The XANES spectrum of the parent compound is characterized by exhibiting a step-like feature at the edge, similar to that of iron metal. The origin of the feature has been succesfully interpreted as due to the hybridization between the $p-d$ conduction empty states at the Fermi level. [54] Hence, although in the K-edge absorption a core electron is removed from the 1s shell and excited to a p-symmetry final state, the existence of the $p-d$ hybridization makes possible to probe, indirectly, the behavior of the magnetic d-states. Upon hydrogen absorption, no significant modification of the XANES resonances is detected, both in energy position and intensity, as expected because the crystal structure of the unhydrided parent compound is retained. [22] However, the differences found in the near-edge region of the absorption spectra corresponding to the $La_2Fe_{14}B$ and $La_2Fe_{14}BH_x$ compounds are noticeably strong at the Fe K-absorption edge. Therefore, the impact of the hydrogen absorption in the crystal structure is rather small, whereas the large differences observed in the edge region address the presence of strong electronic effects induced on Fe atoms.

The present results show that the Fe K-edge threshold is shifted towards higher energies upon H_2 uptake, and that the intensity of the shoulder-like feature at the edge decreases

upon hydrogen absorption. The same behavior is found in $Ce_2Fe_{14}B$ and Ce_2Fe_{17} compounds, as also shown in Fig. 1. Within our experimental resolution, in the case of Ce_2Fe_{17}, both effects are slightly larger for the nitrogen interstitial doped compound as compared with the hydride derivative.

These results reveal the existence of a strong electronic perturbation on the Fe atoms driven by the interstitial doping. Indeed, the shift of the threshold towards higher energy for the interstitial doped compounds can be related to the shift of the Fermi level towards higher energy, while the decrease of the intensity of the shoulder-like resonance at the raising edge indicates that the density of empty p(d) states above the Fermi energy decreases upon H_2(N) uptake. The origin of such a resonance is due to the large $p-d$ hybridization of the conduction bands at the Fermi level, so that the photoelectron finds a large density of dipole allowed delocalized p-like final states. The observed reduction indicates that the local density of $p(d)$-states, projected on the Fe sites, is reduced after the interstitial doping. As a consequence, we can infer from XAS data that the Fermi level shifts towards higher energy and sites in a region with a lower density of states in the case of the hydride(nitride) derivatives.

Based on the above results a deeper insight on the origin of the modification of the magnetic properties induced by hydrogen (nitrogen) in these intermetallic compounds can be obtained. Indeed, upon hydrogen absorption, an increase of the magnetic moment of Fe atoms has been observed in all the R-Fe systems investigated to date. On the contrary, an opposite behavior is found for Co and Ni based compounds. Several mechanisms have been proposed to account for such a controversial behavior. In the case of the $R_2Fe_{14}B$ series, Andreev et al. [55] have proposed that hydrogen uptake leads to the formation of low-energy electron states which are filled by electrons coming from the 3d band. In this scheme, the increase in μ_{Fe} should be due to an increase of the splitting of the $3d$-band, acompanied by a decrease of the Fermi energy. Others authors have interpreted the increase of the Fe magnetic moment as due to the narrowing of the $3d$-band or to the weakening of the $R-Fe$ hybridization upon gas uptake [4,11].

However, the shift towards higher energy of the Fermi level observed by XANES rules out the hypothesis of a low-lying state formation upon interstitial doping. Moreover, this result cannot be understood taking into account, as the only responsible mechanism, a narrowing of the 3*d*-band due to the cell expansion. In fact, it is necessary to consider that the 3*d*-band become gradually filled upon H_2 uptake as early proposed by Kuijpers [56]. The Fe *K*-edge XANES spectra show a similar trend of the Fermi level upon gas uptake in all the systems investigated, so that it sites in a lower density of states (DOS) region independently of both the rare-earth component (La,Ce), and the Fe concentration ($Ce_2Fe_{14}B$, Ce_2Fe_{17}). This result suggests the existence of an interplay between the charge-transfer effect and the decrease of the hybridization between the rare-earth and the Fe conduction bands induced by the interstitial doping. In addition, the shift of the Fermi level in both $La_2Fe_{14}B$ and $Ce_2Fe_{14}B$ systems is similar, whereas the narrowing of the 3*d*-band caused by the crystal-cell expansion is expected to be larger for the Ce-based compound. Moreover, in the case of the Ce_2Fe_{17} derivatives, the shift of the Fermi level is lower than that found in the $R_2Fe_{14}BH_x$ compounds, whereas the crystal-cell expansion is significantly larger. This last result is in agreement with the existence in the latter compounds of more conduction electrons available in the system after the gas absorption.

Finally, it is important to note that for similar hydrogen and nitrogen charging of the Ce_2Fe_{17} compound, while the observed shift of the threshold energy is identical, the decrease of the shoulder-like resonance at the raising edge is markedly larger in the nitride derivative. This result can be related with a larger decrease of the hybridization of the valence electrons of the rare-earth with the 3d electrons of Fe atoms induced by nitrogen. As consequence, the broadening of the 3*d*-band becomes smaller in $Ce_2Fe_{17}N_x$ than in $Ce_2Fe_{17}H_x$ and Ce_2Fe_{17}, enhancing the effective Coulomb repulsion and the band splitting, thus leading to a larger increase of the Fe 3*d* moment in the former compound.

B. L_3-edge XANES spectra: mixed-valence behavior of cerium

Both $Ce_2Fe_{14}B$ and Ce_2Fe_{17} compounds present anomalously small cell-parameters as compared with those of the rest of the repective series. Moreover, according to numerous experimental investigations, Ce atoms do not carry any magnetic moment of $4f$ origin. [57,58] Upon hydrogen and nitrogen absorption, the Ce-based materials suffer the highest cell-expansion in both $R_2Fe_{14}B$ and R_2Fe_{17} series; a trend that has been largely associated to the development of a localized magnetic moment at the Ce sites upon gas charging. [28,35–43]. However, previous XAS experiments performed at the Ce L_3-edge in the hydrides derivatives have shown the inadequacy of such a scheme. [44,45]

The absorption at the L_3-edge of the rare-earth in these compounds constitutes a good challenge to investigate both the impact of the interstitial gas on the $5d$ band and the dynamics of the Ce electronic state. The possibility to probe directly the rare-earth $5d$ band is of fundamental interest in the case of $La_2Fe_{14}B$ and $La_2Fe_{14}H_x$ compounds. Indeed, due to the absence of magnetic moment of $4f$ origin on the La atoms, the $5d$ magnetism is exclusively due to the hybridization of the $5d$ band with the $3d$ band of Fe. Hence, any modification of this $5d-3d$ hybridization, associated with the gas charging, should be reflected on the XANES absorption profile. The XANES spectra at the La L_3-edge in the case of $La_2Fe_{14}B$ and its hydride derivative are shown in Fig. 2. They are characterized by exhibiting a pronounced peak at the absorption threshold, that corresponds to the atomic $2p \rightarrow 5d$ transition (white line). This behavior is common to both rare-earth vapors and metals, indicating that the $5d$ states retain their atomic character upon condensation. In the case of the hydride derivative, the white-line shows two marked changes with respect to that of the unhydrided parent $La_2Fe_{14}B$: it becomes narrower and less intense; and as in the case of the Fe K-edge, the edge is shifted towards higher energy. The second effect reflects the existence of a shift of the Fermi level induced by the injection of more electrons to the conduction bands of the system. On the other hand, the narrowing of the white-line profile reflects a higher localization of the $5d$ band at the La sites and, consequently, the weakening

of the hybridizaton between the La-5d and Fe-3d bands. This picture is also supported by the decrease of the white-line heigth upon hydrogen uptake, indicating the reduction of the d-symmetry empty states at the La sites, as expected if the $3d-5d$ overlap becomes smaller.

In the case of the Ce-based materials, namely $Ce_2Fe_{14}B$ and Ce_2Fe_{17}, the XANES spectra at the Ce L_3-edge show a characteristic double peak reflecting the existence of two configurations in the initial state, $4f^n$ and $4f^{n+1}$, as shown in Fig. 2. This peculiar profile is made by the superposition of the atomic $2p \rightarrow 5d$ transition for each ground state configuration. The white line corresponding to the $4f^{n+1}$ configuration is shifted to lower energy with respect to that of the $4f^n$ due to the screening of the additional $4f$-electron [59]. Therefore, the study of the absorption spectra at the Ce L_3-edge provides an unique tool to determine the electronic state of Ce. In the case of the $Ce_2Fe_{14}B$ and Ce_2Fe_{17}, the XANES spectra indicate that Ce atoms present mixed-valence behavior. The detection of the two configurations in the ground state is possible because the time scale of the absorption process is two to three orders of magnitude smaller than that associated to the valence fluctuation [60]. Moreover, by treating the L_3 absorption as a single-particle process and neglecting final state effects, it is possible to estimate the fractional occupation of the $4f$ configurations in the initial state, i.e., the electronic valence, starting from the intensity ratio of the two white-lines that weight the intensity in the final state. [61] In this way, an estimate for the Ce valence was extracted through the deconvolution of the normalized XANES spectra by using arctangent functions to describe the transitions into the continuum states and Lorentzian functions to take account of the atomic-like $2p \rightarrow 5d$ transitions [61,62]. The deconvolution process was performed using a least square fitting procedure to fit the normalized spectra to this expression:

$$
\begin{aligned}
F(E) = B_0 + B_1 E + \frac{(\frac{\Gamma}{2})^2 A_1}{(E-E_1)^2 + (\frac{\Gamma}{2})^2} + \frac{(\frac{\Gamma}{2})^2 A_2}{(E-E_2)^2 + (\frac{\Gamma}{2})^2} \\
+ \frac{A_1}{A_1 + A_2}\left\{\frac{1}{2} + \frac{1}{\pi}\arctan\left[\frac{E-(E_1+\delta)}{\frac{\Gamma}{2}}\right]\right\} \\
+ \left\{1 - \frac{A_1}{A_1 + A_2}\right\}\left\{\frac{1}{2} + \frac{1}{\pi}\arctan\left[\frac{E-(E_2+\delta)}{\frac{\Gamma}{2}}\right]\right\} \qquad (1)
\end{aligned}
$$

where E_1 and E_2 are respectively the first accessible $5d$-states in $4f^{n+1}$ and $4f^n$ configurations and A_1 and A_2 describe the relative weight of the two configurations. Γ is the core-hole lifetime for the transition and δ is the shift between the onset of the continuum and bound states transitions. B_0 and B_1 are the coefficients of a linear background [44,62].

The deconvolution of the L_3 absorption edge of cerium for $Ce_2Fe_{14}B$ and Ce_2Fe_{17} returns a valence of 3.22 and 3.33 repectively. Upon hydrogen absorption no modification of cerium valence is found for the $Ce_2Fe_{14}B$ compound. On the contrary, both Ce_2Fe_{17} hydride and nitride exhibit a decrease of the Ce valence to 3.22 . Hence, the Ce mixed-valence behavior is retained in all these systems, ruling out the possiblity of the developing of a $4f$ magnetic moment induced by hydrogen (nitrogen) uptake. Our results demonstrate that the strong expansion of the crystal structure in both Ce-based compounds upon gas charging is not linked to the modification of the Ce electronic state. In addition, they constitute an evidence of the weakening of the $3d - 5d$ hybridization induced by both hydrogen and nitrogen absorption.

C. L_1-edge XANES spectra

The previous analyses of the Fe K-edge, Ce and La L_3-edge XANES absorption spectra indicate that the gas charging modifies the overlapping between the conduction bands of both rare-earth and Fe. An additional test of this effect can be obtained by tuning the energy of the absorption at the L_1-edge of the rare-earth elements.

The spectral shape of the L_1 spectra in all the lanthanide metals exhibits a step-like rise of the absorption at the threshold. This feature reflects the p-projected density of states in the band structure of the conduction electrons. In the case of rare-earths vapors, such a structure is absent in the L_1 spectra because the atomic resonances corresponding to the one-electron transition $s - p$ are very weak due to the small oscillator strengths of the $s - p$ transitions [63,64]. However, upon condensation into the metallic state, the L_1 spectra lose their atomic character completely and a shoulder-like feature appears. [65] This behavior is

the experimental evidence that the outer *p*-symmetry orbitals are strongly hybridized with the outer *s*- and *d*-symmetry orbitals in metals, reflecting the high density of empty 5*d* states via hybridization of the R(*sp*) and R(5*d*) empty states. Therefore, the modification of the width and intensity of the shoulder-like near-edge structure is a fingerprint of hybridization changes of the outermost orbitals between the absorbing atom and the nearest neighbors. Actually, in the case of R-Fe intermetallic compounds, due to the strong hybridization between the rare earth 5*d* and Fe-3*d* orbitals, the study of the L_1 absorption spectra provide an unique insight to study the behavior of the R(5*d*)-Fe(3*d*) hybridization upon gas charging.

Fig. 3 shows the comparison of the XANES spectra at the La and Ce L_1-edge in both $La_2Fe_{14}B$ and $Ce_2Fe_{14}B$ and their hydrides derivatives. In both cases, a reduction of the shoulder-like feature is induced by hydrogen absorption, indicating a more localized nature of the $p - d$ orbitals of the rare-earth, similar to the rare-earth vapors case. This result supports the hypothesis that a higher localization of the 5*d* band at the rare earth site takes place upon hydriding, as well as the concomitant reduction of the R(5*d*)-Fe(3*d*) overlap that determines the interplay between the two magnetic sublattices. We have to notice that the narrowing of the shoulder is greater in the $Ce_2Fe_{14}B$ hydride than in the $La_2Fe_{14}B$ one, adressing the anomalous volume expansion of the Ce-based hydride to a higher reduction of the R-Fe hybridization, rather than to a change of the cerium valence, which indeed is not detected in our experiments. Moreover, comparison of the Ce-L_1 XANES spectra of Ce_2Fe_{17} and its hydride and nitride derivatives, shown in Fig. 3, exhibit a huge reduction of the edge-feature upon gas charging, as in the $Ce_2Fe_{14}BH_x$ systems. This reduction is slightly larger for the nitride than for the hydride derivative, also in agreement with the higher volume expansion observed in the former compound.

D. XCMD study in $R_2Fe_{14}BH_x$ systems (R=La, Ce)

From the previuos analyses of the XANES spectra we addressed that the mechanism playing a major role in the modification of the electronic and magnetic properties of the

$La_2Fe_{14}B$, $Ce_2Fe_{14}B$ and Ce_2Fe_{17} systems upon gas charging, is mainly related to the change of the $R-Fe$ hybridization. A further test can be achieved by analyzing the x-ray circular magnetic dichroism (XCMD) at the rare-earth L- and at the Fe K-absorption edges. Indeed, by recording the spin-dependent absorption cross-section is possible to probe the spin polarization of the $5d$ empty states of the rare earth, L_2-edge, and the $4p$ empty states of Fe, K-edge. [66] The XCMD probe is of fundamental interest because allows to characterize magnetically the $5d$ states, that mediate the $4f-3d$ exchange interaction, and thus the magnetic properties of the $R-Fe$ intermetallic compounds.

Fig. 4 shows the comparison of the La L_2-edge XCMD spectra for $La_2Fe_{14}B$ and its hydride derivative. The comparison performed at the iron K-edge is also shown. The spin-dependent absorption coefficient has been obtained as the difference of the absorption coefficient $\mu_c = (\mu^- - \mu^+)$ for parallel, μ^+, and antiparallel, μ^-, orientation of the photon spin and the magnetic field applied to the sample. The L_2 absorption spectrum is sensitive to the $d_{3/2}$ final-state density, and due to the existence of spin-orbit coupling in the initial state, the XCMD spectra are directly related to the spin polarization of the final d states projected on the La site. This fact makes possible to relate the dichroic signal to the magnetic moment carried by the $5d$ electrons. Hence, according to Brouder at al. [67], the XCMD signal at the L_2-edge, defined as above, can be written as

$$\Delta\sigma_{L_2} = \frac{\sigma^-(B) - \sigma^+(B)}{\sigma^+(B) + \sigma^-(B)} = \frac{\sigma^{\uparrow}_{21/2} - \sigma^{\downarrow}_{21/2}}{2(\sigma^{\downarrow}_{21/2} + \sigma^{\uparrow}_{21/2})} \tag{2}$$

where $\sigma^{\uparrow(\downarrow)}_{2j}$ holds for the reduced transition probability towards up (down) spins. Consequently, the analysis of the XCMD spectra would lead to a direct determination of the sign of the magnetic coupling between the La $5d$ and the Fe $3d$ spins. In the case of $La_2Fe_{14}B$ and its hydride derivative XCMD signals are negative at the L_2-edge, indicating that the dominant transitions are those towards minority-spin $5d$-states. According to the simplified model of the level densities for rare-earth transition metal intermetallic compounds developed by Johanson et al. [68], the energy distance between the bonding and antibonding $3d-5d$ subbands is different for the two spin directions and therefore $3d-5d$ hybridization

is different for the majority and minority spins. In the case that no localized $4f$ magnetic moment is present in the system, the occupation of the spin down (minority) of the $5d$ component exceeds that of the spin up (majority) part that is hybridized to the majority spin Fe-$3d$ band. Consequently there is a total $5d$ spin moment on the rare-earth coupled antiferromagnetically to the Fe $3d$ moment.

In the case of $La_2Fe_{14}B$, $Ce_2Fe_{14}B$ and their hydrides, XCMD spectra support the above picture indicating both the existence of an ordered net $5d$ magnetic moment at the La and Ce sites as well as its antiferromagnetic coupling to the Fe $3d$ magnetic moment. This trend agrees with the Campbell's indirect exchange hypothesis formulated to account for the magnetic coupling in rare-earth transition metal compounds [69]. Upon hydriding, the La L_2-edge XCMD signal of the $La_2Fe_{14}B$ increases with respect to that of the parent compound, in agreement with the weakening of the $5d-3d$ ocurred upon H_2 uptake. Indeed, the reduction of the $5d-3d$ hybridization implies a further decrease of the $5d$ content in the bonding band, which is larger for the spin-up component. [68] Consequently, the number of accessible spin-up $5d$-states decreases more than that of the spin-down states, and according to Eq. 2 the XCMD signal should increase upon hydrogen uptake, as confirmed by our experimental results.

The XCMD signal at the Ce L_2-edge in $Ce_2Fe_{14}B$ and its hydride present a double-peak structure that resembles the existence of configurational mixing in the ground state, as in the case of polarization averaged XAS spectra (see Fig. 3). Moreover, the sign of the XCMD is negative as for nonmagnetic rare-earths. [70] On the contrary, in magnetic rare earths the $4f$ states are split into the occupied states, occuring at about -7 eV below E_F, and those unoccupied above the Fermi level [71]. In these cases, although the number of empty spin-up (majority) $5d$-states exceeds that of the minority spin above the Fermi level, the matrix elements for the transition to the spin-down states are larger than to the spin-up states because of the intra-atomic $4f-5d$ overlap. [72–74] As a consequence, the sign of the XCMD has to be positive, as shown in Fig. 4 for the case of $Nd_2Fe_{14}B$ [52]. Therefore, upon developing of a localized Ce $4f$ magnetic moment in the $Ce_2Fe_{14}B$ hydride, a change

of sign of the XCMD should be expected, contrary to the experimental result. [49]

Finally, we briefly comment the behavior of the XCMD signal at the Fe K-edge in the case of $La_2Fe_{14}B$ and its hydride derivative. Both signals are almost identical to that of iron metal [52], and present a narrow positive peak, $\simeq$ 5 eV wide, followed by a broader negative signal. This profile has been accounted for by considering the spin-splitting of the final p-projected states at the Fe site and the hybridization of the $4p$ and $3d$ states. This hybridization modulates the weight of the spin-dependent absorption cross-section for transitions towards spin-up (down) $4p$ states. [67] Furthermore, the sign of the XCMD signal at the Fe sites indicates that the majority of $4p$ spins are antiferromagnetically coupled to the $3d$ spins. [67] Upon hydrogen absorption, the positive peak of the XCMD signal increases whereas the intensity of the deep decreases, reflecting the enhancement of the Fe $3d$ magnetic moment.

E. CONCLUSIONS

The interpretation of the x-ray absorption spectra recorded at the rare-earth $L_{1,3}$-edges and at the Fe K-edge clarifies the origin of the magnetic changes occurred upon hydrogen (nitrogen) uptake in $R_2Fe_{14}B$ (R=La, Ce) and Ce_2Fe_{17} systems.

The analysis of the Fe K-edge and rare-earth L_1 XANES spectra shows the existence of strong electronic effects induced upon gas charging. The interplay between electronic charge transfer to the conduction bands and the weakening of the hybridization between the R $5d$- and the Fe $3d$-states is responsible for the enhancement of the Fe magnetic moment.

Contrary to previous assignements [28,35–43], the mixed-valence behavior of Ce, determined from the L_3-absorption XANES analysis, indicates that upon $H_2(N)$ uptake no development of a localized $4f$ magnetic moment takes place. Claim for the developing of $4f$ magnetic moment in Ce ions upon hydrogen uptake in these compounds has been proposed by establishing a parallel to the isostructural γ-α transition of Ce metal, that exhibits a $\simeq$16% volume collapse and the extinction of the magnetic moment. This assignement that

deals with the concept of a charge transfer from Ce^{4+} to Ce^{3+} ocurred upon gas charging, within the framework of the Zachariasen-Pauling promotional model, involves the promotion of one electron from the $5d$ conduction-band to a well localized $4f$ state. [75] The application of this model to the Ce-based systems, like Ce metal, has been strongly questioned by recent $ab-initio$ electronic structure calculations that show how in α-Ce the unoccupied $4f$-states are strongly hybridized with the $5d$ bands. Consequently, it is the competition between the $f-f$ Coulomb interaction and the $f-d$ hybridization that determines the localization of the $4f$ electrons, the volume and the magnetic state of Ce atoms. [71,76–78]

The results of the present investigation are in full agreement with these calculations, showing direct details of the reduction of the $f-d$ hybridization induced by hydrogen and nitrogen uptake. However, in Ce-based compounds this effect is not enough to determine the localization of the $4f$ states and the subsequent turn up of a $4f$ magnetic moment at the Ce sites, as also clearly demonstrated by x-ray circular magnetic dichroism experiments performed at the same absorption edges. The combined interpretation of unpolarized (XAS) and polarized (XCMD) absorption data support also the hypothesis that the anomalous strong cell expansion of the Ce-based compounds is linked to the sensitivity of Ce to the hybridization between the $4f$ and $5d$ states, directly related to the reduction of the Ce($5d$)-Fe($3d$) overlapping.

ACKNOWLEDGMENTS

This work was partially supported by INFN-CICYT agreement and spanish DGICYT MAT93-0240C04 grant. Valuable discussions with J. Bartolomé and L.M. Garcia are kindly recognized. We wish also to acknowledge T. Murata, H. Kawata, T. Iwazumi and T. Miyahara for experimental support at KEK. A special acknowledgment is devoted to H. Maruyama and K. Kobayashi for their enthusiastic contribution during the experimental runs at KEK and for the clarifying discussion on the XCMD results.

REFERENCES

[1] H. Zijlstra and F.F. Westendorp, Solid State Commun. **7**, 857 (1969).

[2] K.H.J. Buschow, P.C.P. Bouten and A.R. Miedema, Rep. Prog. Phys. **45**, 937 (1982) and references therein.

[3] W.E. Wallace, in *Hydrogen in Metals* Vol. I, edited by G. Alefeld and J. Volkl, Topics in Applied Phys. Vol. 28 (Springer-Verlag, Berlin, 1978) and references therein.

[4] K.H.J. Buschow, in *Handbook on the Physics and Chemistry of Rare Earths*, edited by K.A. Gschneidner Jr. and L. Eyring, Vol. 6, (North-Holland, Amsterdam, 1984) and references therein.

[5] G. Wiesinger and G. Hilscher, in *Handbook of Magnetic Materials*, edited by K.H.J. Buschow, Vol. 6, (Elsevier, Amsterdam, 1991) and references therein.

[6] M. Yamaguchi and E. Akiba, in *Materials Science and Technology*, edited by R.W. Cahn, P. Haasen and E.J. Kramer, Vol. 3B, (VCH, Weinheim, 1994) and references therein.

[7] M. Sagawa, S. Fujimura, M. Togawa, H. Yamamoto and Y. Matsuura, J. Appl. Phys. **55**, 2083 (1984).

[8] J. J. Croat, J.F. Herbst, R.W. Lee and F.E. Pinkerton, J. Appl. Phys. **55**, 2078 (1984).

[9] K.H.J. Buschow, in *Handbook of Magnetic Materials*, edited by E.P. Wohlfarth, Vol. 4, (North-Holland, Amsterdam, 1988) and references therein.

[10] E. Burzo and H.R. Kirchmayr, in *Handbook on the Physics and Chemistry of Rare Earths*, edited by K.A. Gschneidner Jr. and L. Eyring, Vol. 12, (North-Holland, Amsterdam, 1989) and references therein.

[11] J.F. Herbst, Rev. Mod. Phys. **63**, 819 (1991) and references therein.

[12] H.R. Kirchmayr and C.A. Poldy, in *Handbook on the Physics and Chemistry of Rare*

Earths, edited by K.A. Gschneidner Jr. and L. Eyring, Vol. 2, (North-Holland, Amsterdam, 1979) and references therein.

[13] J.J.M. Franse and R.J. Radwanski, in *Handbook of Magnetic Materials*, edited by K.H.J. Buschow, Vol. 7, (North-Holland, Amsterdam, 1993) and references therein.

[14] H.S. Li and J.M.D. Coey, in *Handbook of Magnetic Materials*, edited by K.H.J. Buschow, Vol. 6, (North-Holland, Amsterdam, 1991) and references therein.

[15] K.H.J. Buschow, Phys. Status Solidi **A7**, 199 (1971).

[16] D. Givord and R. Lemaire, IEEE Trans. Magn. **MAG-10**, 109 (1974).

[17] J.P. Gavigan, D. Givord, H.S. Li and J. Voiron, Physica B **149**, 345 (1988)

[18] P. Mohn, E. Wohlfarth, J. Phys. F: Metal Phys. **17**, 2421 (1987).

[19] P. L'Heritier, P. Chaudouet, R. Madar, A. Rouault, J-P. Senateur and R. Fruchart, C.R. Acad. Sci. Ser. II **299**, 849 (1984).

[20] K. Oesterreicher and H. Oesterreicher, Phys. Status Solidi **A 85**, K61 (1984).

[21] F. Pourarian, M.Q. Huang and W.E. Wallace, J. Less Common Met. **120**, 63 (1986).

[22] D. Fruchart, P. Wolfers, P. Vulliet, A. Yaouanc, R. Fruchart and P. L'Heritier, in *Nd-Fe Permanent Magnets. Their Present and Future Applications*, edited by I.V. Mitchell, (Elsevier, Amsterdam,1986).

[23] L.Y. Zhang, F. Pourarian and W.E. Wallace, J. Magn. Magn. Mater. **71**, 203 (1988).

[24] L. Neel, Ann. Phys. (Paris) **5**, 232 (1936).

[25] J. Zufrowski, A. Barnasik, K. Krop, R.J. Radwanski, J. Pszczola, J. Suwalski, Z. Kucharski and M. Lukasiak, Hyper. Inter. **15-16**, 801 (1983).

[26] B. Rupp and G. Wiesinger, J. Magn. Magn. Mater. **61**, 269 (1988).

[27] X.Z. Wang, K. Donelly, J.M.D. Coey, B. Chevalier, J. Etourneau and T. Berlureau, J. Mater. Sci. **23**, 329 (1988).

[28] O. Isnard, S. Miraglia, J.L. Soubeyroux, D. Fruchart and A. Stergiou, J. Less Common Met. **162**, 273 (1990).

[29] D.B. de Mooij and K.H.J. Buschow, J. Less Common Met. **142**, 349 (1988).

[30] X-P. Zhong, R.J. Radwanski, F.R. de Boer, T.H. Jacobs and K.H.J. Buschow, J. Magn. Magn. Mater. **86**, 333 (1990).

[31] H. Sun, B-P. Hu, H-S. Li and J.M.D. Coey, Sol. State Commun. **74**, 727 (1990).

[32] J.M.D. Coey and H. Sun, J. Magn. Magn. Mater. **87**, L251 (1990).

[33] H. Sun, J.M.D. Coey, Y. Otani and D.P.F. Hurley, J. Phys. C: Condens. Matter **2**, 6465 (1990).

[34] Y. Otani, D.P.F. Hurley, H. Sun and J.M.D. Coey, J. Appl. Phys. **69**, 5534 (1991)

[35] P. Dalmas de Reotier, D. Fruchart, L. Pontonnier, F. Vaillant, P. Wolfers, A. Yaouanc, J. M. Coey, R. Fruchart, Ph. L'Heritier, J. Less Common Met. **129**, 133 (1987).

[36] O. Isnard, PhD Thesis, University J. Fourier, Grenoble (1994).

[37] O. Isnard, S. Miraglia, C. Kolbeck, E. Tomey, J.L. Soubeyroux, D. Fruchart, M. Guillot and C. Rillo, J. Alloys and Comp. **178**, 15 (1992).

[38] O. Isnard, S. Miraglia, J.L Souberyoux, D. Fruchart, J. Pannetier, Phys. Rev. **B 45**, 2920 (1992).

[39] D. Fruchart, F. Vaillant, A. Yaouanc, J. M. Coey, R. Fruchart, Ph. L'Heritier, T. Riesterer, J. Osterwalder y L. Schlapbach, J. Less Com. Met. **130**, 97 (1987).

[40] S. Miraglia, M. Anne, H. Vincent, D. Fruchart, J. M. Laurant, M. Rossignol, J. Less Com. Met. **153**, 51 (1989).

[41] O. Isnard, S. Miraglia, J.L. Soubeyroux, D. Fruchart and A. Stergiou, J. Less Common Met. **162**, 273 (1990).

[42] O. Isnard, S. Miraglia, D. Fruchart and J. Deportes, J. Magn. Magn. Mater. **103**, 157 (1992).

[43] O. Isnard, S. Miraglia, C. Kolbeck, E. Tomey, J.L. Soubeyroux, D. Fruchart, M. Guillot and C. Rillo, J. Alloys and Comp. **178**, 15 (1992).

[44] J. Chaboy, PhD Thesis, Zaragoza University (1991).

[45] J. Chaboy, J. Garcia, A. Marcelli, O. Isnard, S. Miraglia and D. Fruchart, J. Magn. Magn. Mater. **104-107**, 1171 (1992).

[46] T.W. Capehart, R.K. Mishra, G.P. Meisner, C. D. Fuerst and J.F. Herbst, App. Phys. Lett. 63, 3642 (1993)

[47] K.H.J. Buschow and A.M. van Diepen, Solid State Commun. **19**, 79 (1976).

[48] J. Chaboy, J. Garcia and A. Marcelli, J. Magn. Magn. Mater. **104-107**, 661 (1992).

[49] J. Chaboy, A. Marcelli, L.M. Garcia, J. Garcia, H. Maruyama, K. Kobayashi and L. Bozukov, Sol. State Commun. **91**, 769 (1994).

[50] J. Chaboy, A. Marcelli and L. Bozukov, Jap. J. Appl. Phys. **32**, 758 (1993).

[51] J. Chaboy, A. Marcelli, L. Bozukov, F. Baudelet, E. Dartyge, A. Fontaine and S. Pizzini, Phys. Rev. B, (in press)

[52] J. Chaboy, A. Marcelli, L.M. Garcia, J. Bartolome, M. Kuzmin, H. Maruyama, K. Kobayashi, H. Kawata and T. Iwazumi, Europhys. Lett., (in press) and LNF-94/016 (P) internal report (1994).

[53] See for example, D.E. Sayers and B.A. Bunker, in *X-ray Absorption: Principles, Applications, Techniques of EXAFS, SEXAFS and XANES*, edited by D.C. Koningsberger

and R. Prins, (John Wiley Sons, New York, 1988) Chap. 6.

[54] A. Bianconi, in *X-ray Absorption: Principles, Applications, Techniques of EXAFS, SEXAFS and XANES*, edited by D.C. Koningsberger and R. Prins, (John Wiley & Sons, New York, 1988) Chap. 11 and references therein.

[55] A.V. Andreev, A.V. Deryagin, N.V. Kudrevatykh, N.V. Mushnikov, V.A. Reimer and S.V. Terent'ev, Sov. Phys. JETP **63**, 608 (1986).

[56] F.A. Kuijpers, Philips Res. Repts. Suppl. **2**, (1973).

[57] W.B. Yelon and J.F. Herbst, J. Appl. Phys. **59**, 93 (1986). For a review, see also Refs. [9-11].

[58] K.H.J. Buschow and J.S. Van Wieringen, Phys. Status Solidi **42**, 231 (1970). For a review, see also Refs. [12-13].

[59] S.M. Blokhin and E. Ye. Vaynshteyn, Fiz. Met. Metaloved., **19**, 371 (1965).

[60] H. Launois, M. Rawiso, E. Holland-Moritz, R. Pott and D. Wohlleben, Phys. Rev. Lett. **44**, 1271 (1980).

[61] J. Röhler, in *Handbook on the Physics and Chemistry of Rare Earths*, edited by K.A. Gschneidner Jr. and L. Eyring and S. Hufner, Vol. 10, (North-Holland, Amsterdam, 1987).

[62] J. Röhler, J. Magn. Mag. Mat. 47&48 175 (1985).

[63] G. Materlik, J.E. Müller and J.W. Wilkins, Phys. Rev. Lett. **50**, 267 (1983).

[64] J.E. Müller and J.W. Wilkins, Phys. Rev. **B29**, 4331 (1984).

[65] G. Materlik, B. Sonntag and M. Tausch, Phys. Rev. Lett. **51**, 1300 (1983).

[66] G. Schütz, W. Wagner, W. Wilhelm, P. Kienle, R. Zeller, R. Frahm and G. Materlik, Phys. Rev. Lett. **58**, 737 (1987); For a review see, S.W. Lovesey, Rept. Prog. Phys. 56,

257 (1993)

[67] C. Brouder and M. Hikam, Phys. Rev. **B43**, 3089 (1991).

[68] B. Johanson, L. Nordström, O. Eriksson and M.S.S. Brooks, Physica Scripta **T39**, 100 (1991).

[69] I.A. Campbell, J. Phys. **F2**, L47 (1972).

[70] C. Giorgetti, S. Pizzini, E. Dartyge, A. Fontaine, F. Baudelet, C. Brouder, Ph. Bauer, G. Krill, S. Miraglia, D. Fruchart and J.P. Kappler, Phys. Rev. **B 48**, 12732 (1993)

[71] Z. Szotek, W.M. Temmerman and H. Winter, Phys. Rev. Lett. **72**, 1244 (1994).

[72] B.N. Harmon and A.J. Freeman, Phys. Rev. **B 10**, 1979 (1974).

[73] X. Wang, T.C. Lueng, B.N. Harmon and P. Carra, Phys. Rev. **B 47**, 9087 (1993).

[74] J.C. Lang, X. Wang, V.P. Antropov, B.N. Harmon, A.I. Goldman, H. Wan, G.C. Hadjipanayis and K.D. Finkelstein, Phys. Rev. **B 49**, 5993 (1994)

[75] W.H. Zachariasen, quoted by A. W. Lawson and T.Y Tang, Phys. Rev. **76**, 301 (1949); L. Pauling, quoted by A.F. Schuck and J. H. Sturdivant, J. Chem. Phys. **18**, 145 (1950).

[76] O. Eriksson, L. Nördstrom, M.S.S. Brooks and B. Johansson, Phys. Rev. Lett. **60**, 2523 (1988).

[77] O. Eriksson, M.S.S. Brooks and B. Johanson, Phys. Rev. **B 41**, 7311 (1990)

[78] A. Svane, Phys. Rev. Lett. **72**, 1248 (1994).

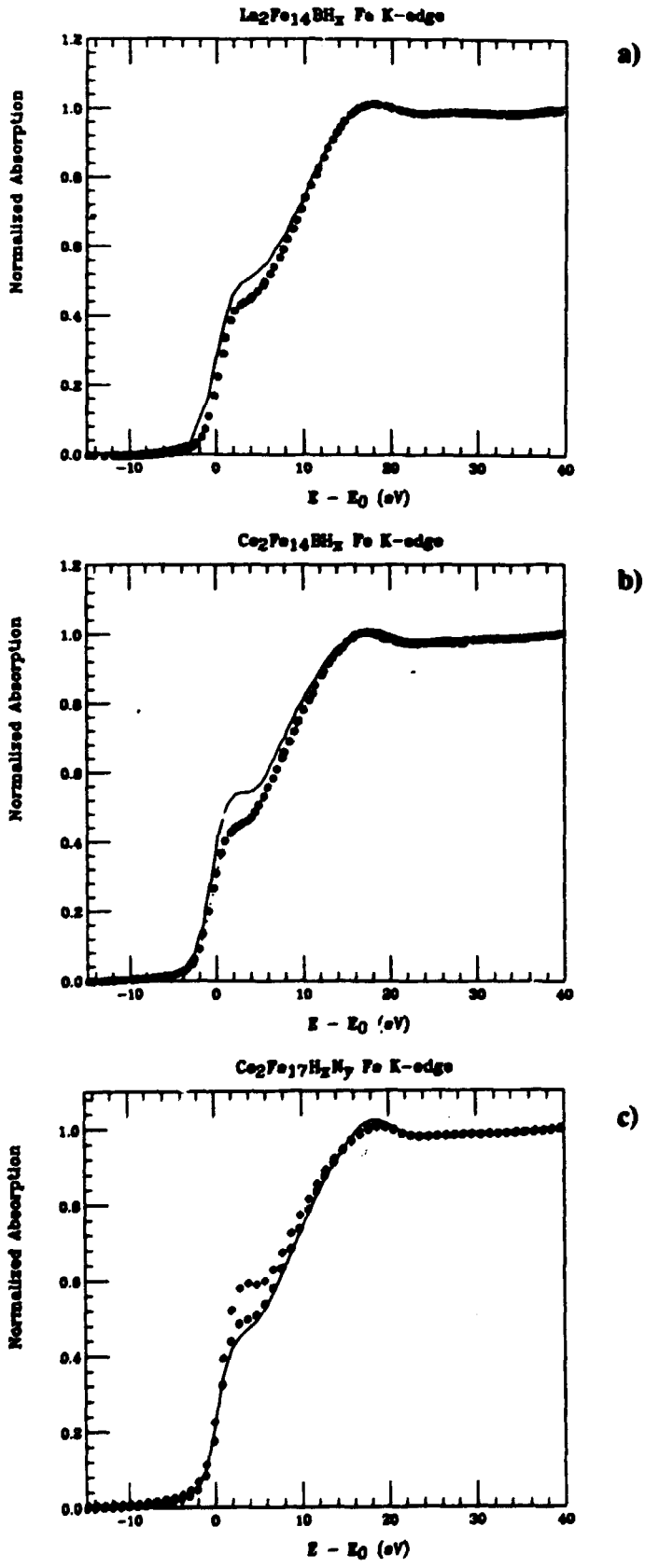

FIG. 1 – Comparison between the experimental XANES spectra at the Fe K-edge in the case of (a) $La_2Fe_{14}B$ (solid) and its hydride derivative (dots); (b) $Ce_2Fe_{14}B$ (solid) and $Ce_2Fe_{14}BH_x$ (dots); (c) Ce_2Fe_{17} (◊), $Ce_2Fe_{17}H_x$ (dots) and the nitride $Ce_2Fe_{17}N_x$ (solid).

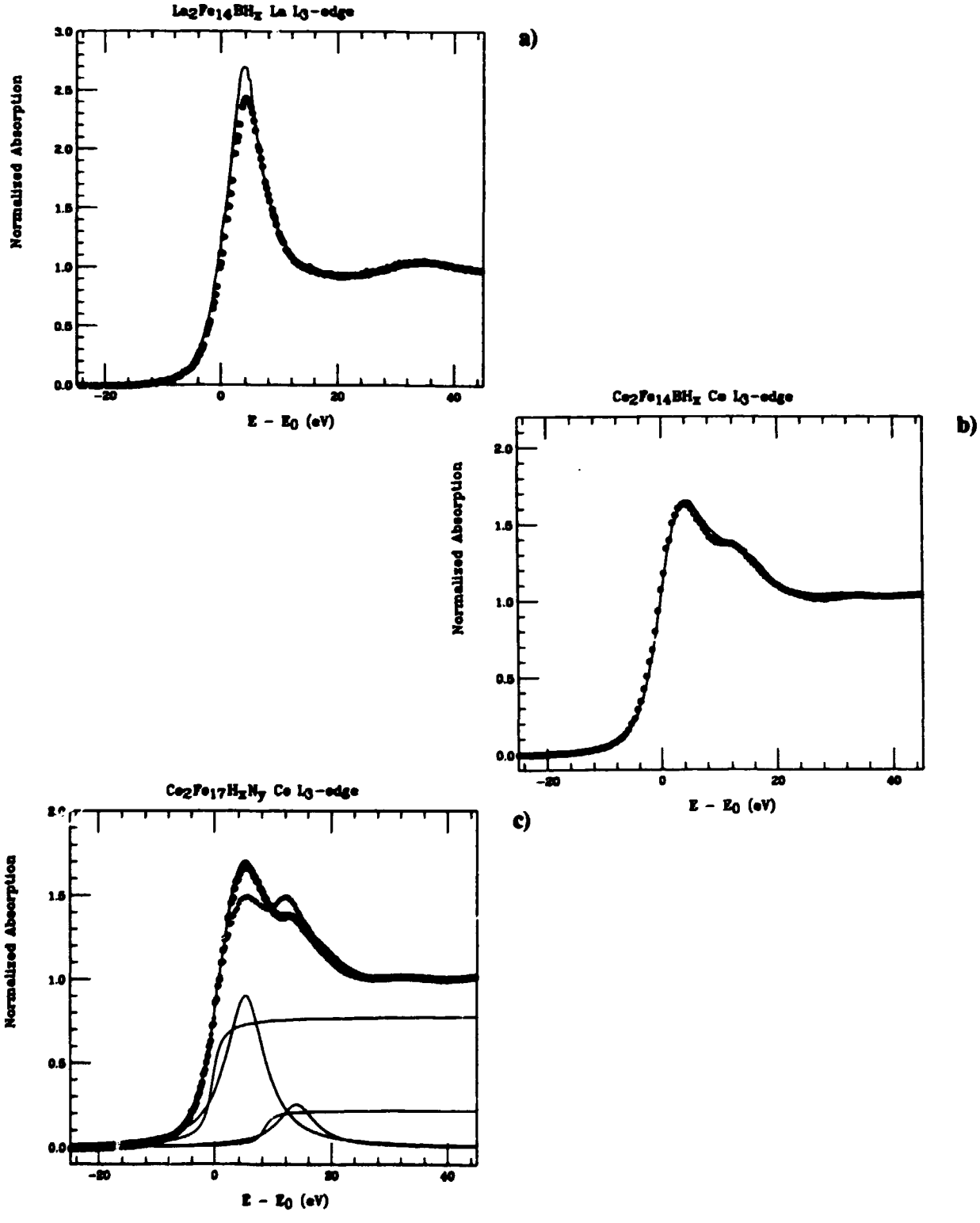

FIG. 2 – a) Comparison between the La L_3-edge XANES spectra for $La_2Fe_{14}B$ (solid) and $La_2Fe_{14}BH_x$ (dots); (b) Normalized Ce L_3-edge XANES spectra in the case of $Ce_2Fe_{14}B$ (solid) and its hydride derivative (dots); (c) Comparison among Ce_2Fe_{17} (◊), $Ce_2Fe_{17}H_x$ (dots) and $Ce_2Fe_{17}N_y$ (solid) compounds. In the same figure is shown, as an example, the deconvolution of the Ce L_3-edge absorption spectrum in the Ce_2Fe_{17} system. The deconvolution has been performed including two arctangent and two Lorentzian functions according to Eq. [1] in the text.

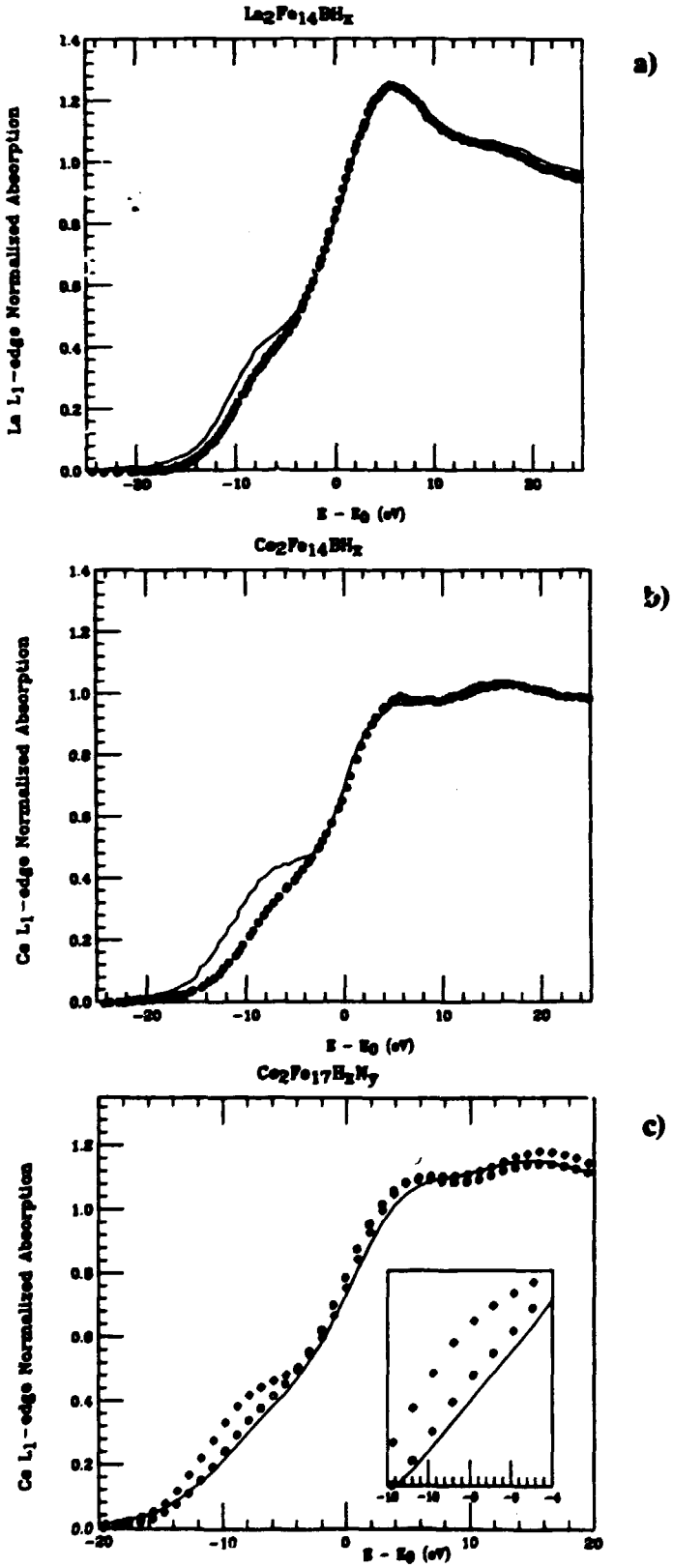

FIG. 3 – Comparison between the experimental XANES spectra at the rare-earth L_1-edge in the case of: (a) $La_2Fe_{14}B$ (solid) and $La_2Fe_{14}BH_x$ (dots); (b) $Ce_2Fe_{14}B$ (solid) and $Ce_2Fe_{14}BH_x$ (dots); (c) Ce_2Fe_{17} (◊), $Ce_2Fe_{17}H_x$ (dots) and the $Ce_2Fe_{17}N_x$ (solid). The inset reports the differences of the near-edge region for the hydride and nitride derivatives.

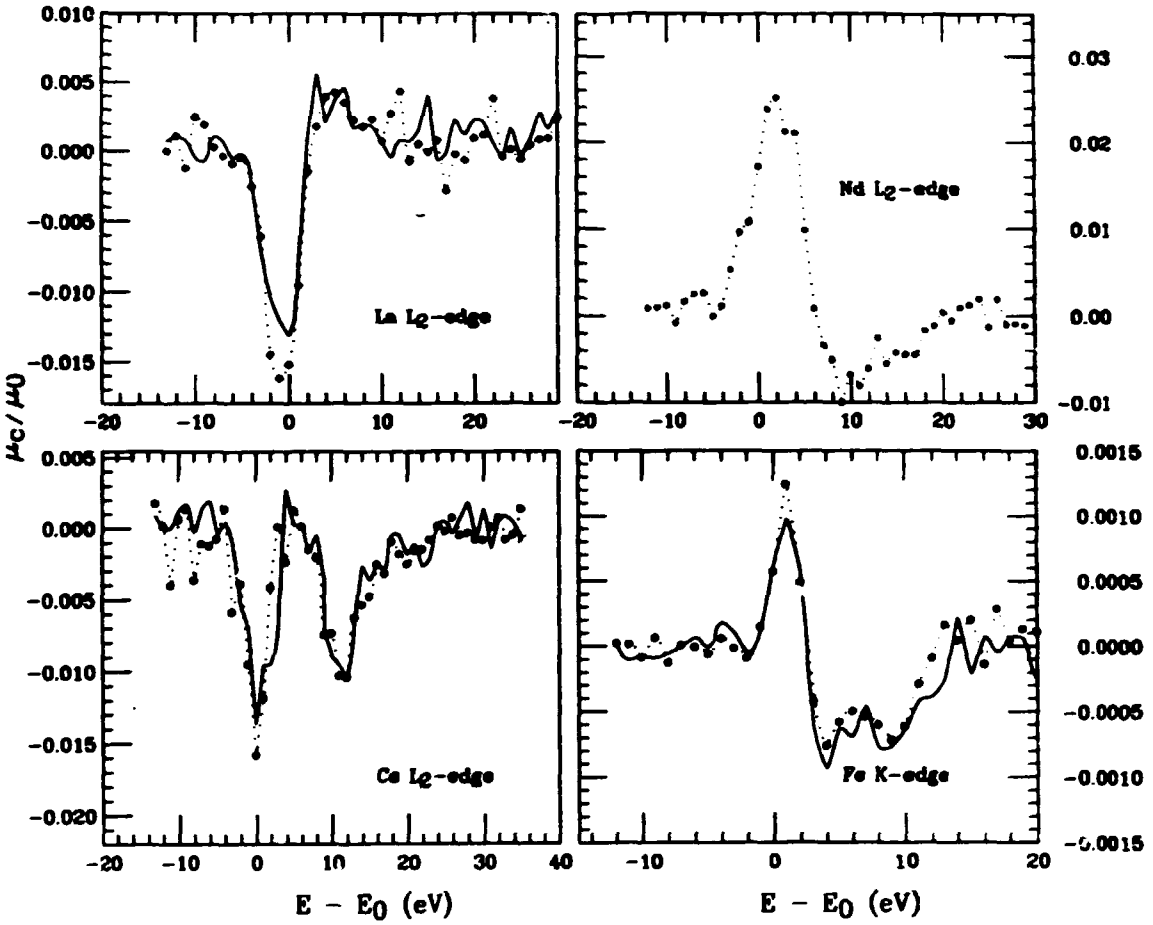

FIG. 4 – XCMD signals at the Fe K–edge (bottom right) and La L_2–edge (top left) of $La_2Fe_{14}B$ (solid) and $La_2Fe_{14}BH_x$ (dots). Comparison is also shown for the XCMD signals at the Ce L_2–edge (bottom left) of $Ce_2Fe_{14}B$ (solid) and $Ce_2Fe_{14}BH_x$ (dots). The Nd L_2–edge XCMD signal of $Nd_2Fe_{14}B$ is also shown in the top right panel.

L T324

95 10 30